

1 **Flip Distance Between Triangulations of a Simple Polygon is**  
2 **NP-Complete**

3 **Oswin Aichholzer · Wolfgang Mulzer ·**  
4 **Alexander Pilz**

5  
6 the date of receipt and acceptance should be inserted later

7 **Abstract** Let  $T$  be a triangulation of a simple polygon. A *flip* in  $T$  is the operation  
8 of replacing one diagonal of  $T$  by a different one such that the resulting graph is again  
9 a triangulation. The *flip distance* between two triangulations is the smallest number  
10 of flips required to transform one triangulation into the other. For the special case of  
11 convex polygons, the problem of determining the shortest flip distance between two  
12 triangulations is equivalent to determining the rotation distance between two binary  
13 trees, a central problem which is still open after over 25 years of intensive study.

14 We show that computing the flip distance between two triangulations of a simple  
15 polygon is NP-hard. This complements a recent result that shows APX-hardness of  
16 determining the flip distance between two triangulations of a planar point set.

---

O. Aichholzer and A. Pilz are supported by the ESF EUROCORES programme EuroGIGA - ComPoSe, Austrian Science Fund (FWF): I 648-N18. W. Mulzer is supported in part by DFG project MU/3501/1. Part of this work was done while A. Pilz was recipient of a DOC-fellowship of the Austrian Academy of Sciences at the Institute for Software Technology, Graz University of Technology, Austria. Preliminary versions appeared as O. Aichholzer, W. Mulzer, and A. Pilz, *Flip Distance Between Triangulations of a Simple Polygon is NP-Complete* in Proc. 29th EuroCG, pp. 115–118, 2013, and in Proc. 21st ESA, pp. 13–24, 2013 [2, 3].

---

O. Aichholzer · A. Pilz (✉)

Institute for Software Technology, Graz University of Technology, Austria.

Tel.: +43-316-873-5732

Fax: +43-316-873-5706

E-mail: [oach|apilz]@ist.tugraz.at

W. Mulzer

Institut für Informatik, Freie Universität Berlin, Germany.

E-mail: mulzer@inf.fu-berlin.de

17 **Keywords** triangulations · flip distance · simple polygon

18 **Mathematics Subject Classification (2000)** 68U05

## 19 **1 Introduction**

20 Let  $P$  be a simple polygon in the plane, that is, a closed region bounded by a piece-  
21 wise linear, simple cycle. A *triangulation* of  $P$  is a geometric (straight-line) maximal  
22 outerplanar graph whose outer face is the complement of  $P$  and whose vertex set consists  
23 of the vertices of  $P$ . The edges that are not on the outer face are called *diagonals*. Let  $d$   
24 be a diagonal whose removal creates a convex quadrilateral. Replacing  $d$  with the other  
25 diagonal of the quadrilateral yields another triangulation of  $P$ . This operation is called  
26 a *flip*. The *flip graph* of  $P$  is the abstract graph whose vertices are the triangulations  
27 of  $P$  and in which two triangulations are adjacent if and only if they differ by a single  
28 flip. We study the *flip distance*, i.e., the minimum number of flips required to transform  
29 a given source triangulation into a target triangulation.

30 Edge flips became popular in the context of Delaunay triangulations. Lawson [15]  
31 proved that any triangulation of a planar  $n$ -point set can be transformed into any other  
32 by  $O(n^2)$  flips. Hence, for every planar  $n$ -point set the flip graph is connected with diam-  
33 eter  $O(n^2)$ . Later, Lawson showed that in fact every triangulation can be transformed  
34 to the Delaunay triangulation by  $O(n^2)$  flips that locally fix the Delaunay property [16].  
35 Hurtado, Noy, and Urrutia [11] gave an example where the flip distance is  $\Omega(n^2)$ , and  
36 they showed that the same bounds hold for triangulations of simple polygons. They  
37 also proved that if the polygon has  $k$  reflex vertices, then the flip graph has diameter  
38  $O(n + k^2)$ . In particular, the flip graph of any planar polygon has diameter  $O(n^2)$ . Their  
39 result also generalizes the well-known fact that the flip distance between any two tri-  
40 angulations of a convex polygon is at most  $2n - 10$ , for  $n > 12$ . This was shown by  
41 Sleator, Tarjan, and Thurston [22] in their work on the flip distance in convex poly-  
42 gons. The latter case is particularly interesting due to the correspondence between flips  
43 in triangulations of convex polygons and rotations in binary trees: The dual graph of  
44 such a triangulation is a binary tree, and a flip corresponds to a rotation in that tree;  
45 conversely, for every binary tree, a triangulation can be constructed.

46 We mention two further remarkable results on flip graphs for point sets. Hanke,  
47 Ottmann, and Schuierer [10] showed that the flip distance between two triangulations is

48 bounded by the number of crossings in their overlay. Eppstein [9] gave a polynomial-time  
49 algorithm for calculating a lower bound on the flip distance. His bound is tight for point  
50 sets with no empty 5-gons; however, except for small instances, such point sets are not  
51 in general position (i.e., they must contain collinear triples) [1]. A recent survey on flips  
52 is provided by Bose and Hurtado [4].

53 Recently, the problem of finding the flip distance between two triangulations of a  
54 point set was shown to be NP-hard by Lubiw and Pathak [18] and, independently, by  
55 Pilz [19]. The latter proof was later improved to show APX-hardness of the problem. A  
56 recent preprint shows that the problem is fixed-parameter tractable [14]. Here, we show  
57 that the corresponding problem remains NP-hard even for simple polygons. This can  
58 be seen as a further step towards settling the complexity of deciding the flip distance  
59 between triangulations of convex polygons or, equivalently, the rotation distance between  
60 binary trees. This variant of the problem was probably first addressed by Culik and  
61 Wood [7] in 1982 (showing a flip distance of  $2n - 6$ ) in the context of similarity measures  
62 between trees.

63 We now give the formal problem definition: given a simple polygon  $P$ , two triangula-  
64 tions  $T_1$  and  $T_2$  of  $P$ , and an integer  $l$ , decide whether  $T_1$  can be transformed into  $T_2$  by  
65 at most  $l$  flips. We call this decision problem POLYFLIP. To show NP-hardness, we give  
66 a polynomial-time reduction from the problem RECTILINEAR STEINER ARBORESCENCE  
67 to POLYFLIP. RECTILINEAR STEINER ARBORESCENCE was shown to be NP-hard by Shi  
68 and Su [21]. In Section 2, we describe the problem in detail. We present the well-known  
69 *double chain* (used by Hurtado, Noy, and Urrutia [11] for giving their lower bound), a  
70 major building block in our reduction, in Section 3. Finally, in Section 4, we describe  
71 our reduction and prove that it is correct.

## 72 2 The Rectilinear Steiner Arborescence Problem

73 Let  $S$  be a set of  $N$  points in the plane whose coordinates are nonnegative integers.  
74 The points in  $S$  are called *sinks*. A *rectilinear tree*  $A$  is a connected acyclic collection of  
75 horizontal and vertical line segments that intersect only at their endpoints. The *length*  
76 of  $A$  is the total length of all segments in  $A$  (cf. [13, p. 205]). The tree  $A$  is a *rectilinear*  
77 *Steiner tree* for  $S$  if every sink in  $S$  appears as an endpoint of a segment in  $A$ . We call  $A$   
78 a *rectilinear Steiner arborescence* (RSA) for  $S$  if (i)  $A$  is rooted at the origin; (ii) every

79 leaf of  $A$  lies at a sink in  $S$ ; and (iii) for each  $s = (x_s, y_s) \in S$ , the length of the path  
 80 in  $A$  from the origin to  $s$  equals  $x_s + y_s$ , i.e., all edges in  $A$  point north or east, as seen  
 81 from the origin [20]. In the problem RECTILINEAR STEINER ARBORESCENCE, we are  
 82 given a set of sinks  $S$  and an integer  $k$ . The question is whether there is an RSA for  $S$   
 83 of length at most  $k$ . Shi and Su showed that RECTILINEAR STEINER ARBORESCENCE  
 84 is strongly NP-complete; in particular, it remains NP-complete if  $S$  is contained in an  
 85  $n \times n$  grid, with  $n$  polynomially bounded in  $N$ , the number of sinks [21].<sup>1</sup>

86 We will need the following important structural property of the RSA. Let  $A$  be an  
 87 RSA for a set  $S$  of sinks. Let  $e$  be a vertical segment in  $A$  that does not contain a sink.  
 88 Suppose there is a horizontal segment  $f$  incident to the upper endpoint  $a$  of  $e$ . Since  $A$   
 89 is an arborescence,  $a$  is the left endpoint of  $f$ . Suppose further that  $a$  is not the lower  
 90 endpoint of another vertical edge. Take a copy  $e'$  of  $e$  and translate it to the right until  $e'$   
 91 hits a sink or another segment endpoint (this will certainly happen at the right endpoint  
 92 of  $f$ ); see Fig. 1. The segments  $e$  and  $e'$  define a rectangle  $R$ . The upper and left side of  $R$   
 93 are completely covered by  $e$  and (a part of)  $f$ . Since  $a$  has only two incident segments,  
 94 every sink-root path in  $A$  that goes through  $e$  or  $f$  contains these two sides of  $R$ , entering  
 95 the boundary of  $R$  at the upper right corner  $d$  and leaving it at the lower left corner  $b$ .  
 96 We reroute every such path at  $d$  to continue clockwise along the boundary of  $R$  until it  
 97 meets  $A$  again (this certainly happens at  $b$ ), and we delete  $e$  and the part of  $f$  on  $R$ .  
 98 In the resulting tree we subsequently remove all unnecessary segments (this happens if  
 99 there are no more root-sink paths through  $b$ ) to obtain another RSA  $A'$  for  $S$ . Then  $A'$   
 100 is not longer than  $A$ . This operation is called *sliding  $e$  to the right*. If similar conditions  
 101 apply to a horizontal edge, we can *slide it upwards*. The *Hanan grid* for a point set is  
 102 the set of all vertical and horizontal lines through its points. Through repeated segment  
 103 slides in a shortest RSA, one can obtain the following theorem.

104 **Theorem 2.1** ([20]) *Let  $S$  be a set of sinks. There is a minimum-length RSA  $A$  for  $S$*   
 105 *such that all segments of  $A$  are on the Hanan grid for  $S \cup \{(0, 0)\}$ .* □

106 We use a restricted version of RECTILINEAR STEINER ARBORESCENCE, called YRSA.  
 107 An instance  $(S, k)$  of YRSA differs from an instance for RECTILINEAR STEINER AR-  
 108 BORESCENCE in that we require that no two sinks in  $S$  have the same  $y$ -coordinate.

109 **Theorem 2.2** *YRSA is strongly NP-complete.*

<sup>1</sup> Although a polynomial-time algorithm was claimed [23], it has later been shown to be incorrect [20].

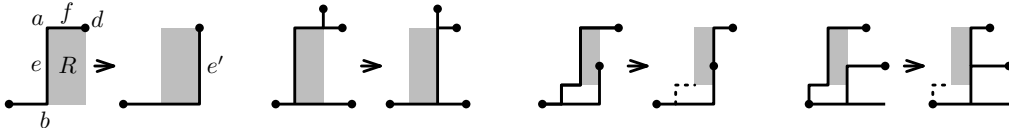


**Fig. 1** The slide operation. The dots depict sinks; the rectangle  $R$  is drawn gray. The dotted segments are deleted, since they do no longer lead to a sink.

110 *Proof* Due to Theorem 2.1, YRSA and RECTILINEAR STEINER ARBORESCENCE are in  
 111 NP [21]. We now show how to transform an instance  $(S, k)$  of RECTILINEAR STEINER  
 112 ARBORESCENCE to an instance of YRSA. We may assume that  $N = |S| \geq 3$ , and we  
 113 number the sinks as  $S = \langle s_1, s_2, \dots, s_N \rangle$  in an arbitrary fashion. For  $i = 1, \dots, N$ ,  
 114 let  $(x_i, y_i)$  be the coordinates of  $s_i$  and define  $s'_i := (x_i N^4, y_i N^4 + i)$ . We set  $S' :=$   
 115  $\{s'_1, s'_2, \dots, s'_N\}$ . The  $y$ -coordinates of the sinks in  $S'$  are pairwise distinct. We will show  
 116 that there is an RSA for  $S$  of length at most  $k$  if and only if there is an RSA for  $S'$  of  
 117 length at most  $kN^4 + N^3$ .

118 Let  $A$  be a rectilinear Steiner arborescence for  $S$  of length at most  $k$ . We scale  $A$  by  
 119  $N^4$  and draw a vertical segment from each leaf to the sink in  $S'$  above it. This gives an  
 120 RSA for  $S'$  of length at most  $kN^4 + N^2 < kN^4 + N^3$ .

121 Conversely, let  $A'$  be an RSA for  $S'$  of length at most  $kN^4 + N^3$ . Due to Theorem 2.1,  
 122 we can assume that  $A'$  is on the Hanan grid. We round the  $y$ -coordinate of every segment  
 123 endpoint in  $A'$  down to the next multiple of  $N^4$  (possibly removing segments of length 0).  
 124 The resulting drawing remains connected; every path to the origin remains monotone;  
 125 and since the segments of  $A'$  lie on the Hanan grid of  $S' \cup \{(0, 0)\}$ , no new cycles are  
 126 introduced. Thus, the resulting drawing constitutes an arborescence  $A''$  for the set  $S''$   
 127 of sinks obtained by scaling  $S$  by  $N^4$ . Since  $A'$  lies on the Hanan grid, it is a union  
 128 of  $N$  paths, each with at most  $N$  vertical segments. The rounding operation increases  
 129 the length of each such vertical segment by at most  $N$ . Thus, the total length of  $A''$  is  
 130 at most  $kN^4 + 2N^3$ . By Theorem 2.1 there exists an optimum arborescence  $A^*$  for  $S''$   
 131 that lies on the Hanan grid. The length of  $A^*$  is a multiple of  $N^4$ , and thus at most  
 132  $kN^4$ , since  $2N^3 < N^4$  for  $N \geq 3$ . It follows that  $S$  has an RSA of length at most  $k$ .

133 Therefore,  $(S, k)$  is a yes-instance for RECTILINEAR STEINER ARBORESCENCE if and  
 134 only if  $(S', kN^4 + N^3)$  is a yes-instance for YRSA. Since  $(S', kN^4 + N^3)$  can be computed  
 135 in polynomial time from  $(S, k)$ , and since the coordinates in  $S'$  are polynomially bounded  
 136 in the coordinates of  $S$ , it follows that YRSA is strongly NP-complete.  $\square$

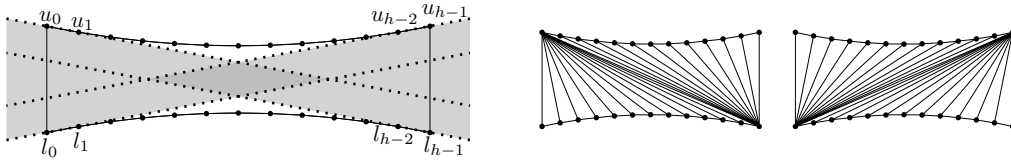


**Fig. 2** Left: The polygon and the hourglass (gray) of a double chain. The diamond-shaped flip-kernel can be extended arbitrarily by flattening the chains. Right: The upper extreme triangulation  $T_u$  and the lower extreme triangulation  $T_l$ .

137 Due to Theorem 2.1, we get the following technical corollary, which will be useful  
138 later.

139 **Corollary 2.3** *YRSA remains strongly NP-complete even if the sinks have coordinates*  
140 *that are a multiple of a positive integer whose value is polynomial in  $N$ .*

### 141 3 Double Chains

142 Our definitions (and illustrations) follow [19]. A *double chain*  $D$  is a polygon that con-  
143 sists of two chains, an *upper chain* and a *lower chain*. There are  $h$  vertices on each chain,  
144  $\langle u_0, \dots, u_{h-1} \rangle$  on the upper chain and  $\langle l_0, \dots, l_{h-1} \rangle$  on the lower chain, both numbered  
145 from left to right, and  $D$  is defined by  $\langle l_0, \dots, l_{h-1}, u_{h-1}, \dots, u_0 \rangle$ . Any point on one chain  
146 sees every point on the other chain, and any quadrilateral formed by three vertices of  
147 one chain and one vertex of the other chain is non-convex; see Fig. 2 (left). We call the  
148 triangulation  $T_u$  of  $D$  where  $u_0$  has maximum degree the *upper extreme triangulation*;  
149 observe that this triangulation is unique. The triangulation  $T_l$  of  $D$  where  $l_0$  has max-  
150 imum degree is called the *lower extreme triangulation*. The two extreme triangulations  
151 are used to show that the diameter of the flip graph is quadratic; see Fig. 2 (right).

152 **Theorem 3.1 (Hurtado, Noy, Urrutia [11])** *The flip distance between  $T_u$  and  $T_l$*   
153 *is  $(h - 1)^2$ .  $\square$*

154 Through a slight modification of  $D$ , we can make the flip distance between the upper  
155 and the lower extreme triangulation linear. This will enable us in our reduction to impose  
156 a certain structure on short flip sequences. To describe this modification, we first define  
157 the *flip-kernel* of a double chain.

158 Let  $W_1$  be the wedge defined by the lines through  $u_0u_1$  and  $l_0l_1$  whose interior  
159 contains no vertex of  $D$  but intersects the segment  $u_0l_0$ . Define  $W_h$  analogously by the

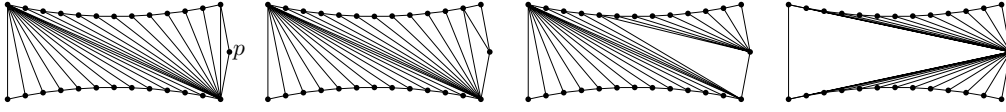


**Fig. 3** The extra point  $p$  in the flip-kernel of  $D$  allows flipping one extreme triangulation of  $Q$  to the other in  $4h - 4$  flips.

160 lines through  $u_{h-1}u_{h-2}$  and  $l_{h-1}l_{h-2}$ . We call  $W := W_1 \cup W_h$  the *hourglass* of  $D$ . The  
 161 unbounded set  $W \cup D$  is defined by four rays and the two chains. The *flip-kernel* of  $D$  is  
 162 the intersection of the four closed half-planes below the lines through  $u_0u_1$  and  $u_{h-2}u_{h-1}$   
 163 and above the lines through  $l_0l_1$  and  $l_{h-2}l_{h-1}$ .<sup>2</sup>

164 **Definition 3.2** Let  $D$  be a double chain and let  $p$  be a point in the flip-kernel  
 165 of  $D$  to the right of the directed line  $l_{h-1}u_{h-1}$ . The polygon given by the sequence  
 166  $\langle l_0, \dots, l_{h-1}, p, u_{h-1}, \dots, u_0 \rangle$  is called a *double chain extended by  $p$* . The upper and the  
 167 lower extreme triangulation of such a polygon contain the edge  $u_{h-1}l_{h-1}$  as a diagonal  
 168 and are otherwise defined in the same way as for  $D$ .

169 The flip distance between the two extreme triangulations of  $D$  extended by a point  $p$   
 170 is much smaller than for  $D$  [24]. Fig. 3 shows how to transform them into each other  
 171 with  $4h - 4$  flips. The next lemma shows that this is optimal, even for more general  
 172 polygons. The lemma is a slight generalization of a lemma by Lubiw and Pathak [18] on  
 173 double chains of constant size.

174 **Lemma 3.3** Suppose that  $h \geq 5$  and consider a polygon that contains  $D$  and has  
 175  $\langle l_0, \dots, l_{h-1} \rangle$  and  $\langle u_{h-1}, \dots, u_0 \rangle$  as part of its boundary. Let  $T_1$  and  $T_2$  be two triangula-  
 176 tions that contain the upper extreme triangulation and the lower extreme triangulation  
 177 of  $D$  as a sub-triangulation, respectively. Then  $T_1$  and  $T_2$  have flip distance at least  
 178  $4h - 4$ .

179 *Proof* We slightly generalize a proof by Lubiw and Pathak [18] for double chains of  
 180 constant size.

181 Let  $C_u$  be the upper chain and  $C_l$  be the lower chain of  $D$ . The triangulation  $T_1$  has  
 182  $2(h - 1)$  triangles with an edge on  $C_u$  or on  $C_l$ . These triangles are called *anchored*, and  
 183 the vertex not incident to the edge on  $C_u$  or on  $C_l$  is called the *apex*. For each anchored  
 184 triangle with an edge on  $C_u$ , the apex must move from  $l_{h-1}$  to  $l_0$ , and similarly for  $C_l$ .

<sup>2</sup> The flip-kernel of  $D$  might not be completely inside the polygon  $D$ . This is in contrast to the “visibility kernel” of a polygon.

185 We distinguish three types of flips depending on whether the convex quadrilateral whose  
 186 diagonal is flipped has (1) four; (2) three; or (3) at most two vertices on  $D$ . A flip of  
 187 type (1) moves the apex of two anchored triangles by one; a flip of type (2) moves the  
 188 apex of one anchored triangle from  $D$  to a point outside  $D$  or back again; and a flip of  
 189 type (3) does not move any apex of an anchored triangle along  $D$  or between a vertex  
 190 of  $D$  and a vertex not in  $D$ .

191 We say that an anchored triangle is of type (1) if its apex is moved only by flips of  
 192 type (1). It is of type (2) if its apex is moved by at least one flip of type (2). Every  
 193 anchored triangle is either of type (1) or of type (2). A type (1) triangle must be involved  
 194 in at least  $h - 1$  flips of type (1), and each of these flips can affect at most one other  
 195 type (1) triangle. A type (2) triangle must be involved in at least 2 flips of type (2), and  
 196 each of these flips can affect no other anchored triangle. Thus, if we have  $m_1$  type (1)  
 197 triangles and  $m_2$  type (2) triangles, we need at least  $(h - 1)m_1/2 + 2m_2$  flips. For  $h \geq 5$ ,  
 198 we have  $(h - 1)m_1/2 + 2m_2 \geq 2(m_1 + m_2) = 4h - 4$ , as claimed.  $\square$

199 The following result can be seen as a special case of [19, Proposition 1].

200 **Lemma 3.4** *Consider a polygon that contains  $D$  and has  $\langle u_{h-1}, \dots, u_0, l_0, \dots, l_{h-1} \rangle$  as  
 201 part of its boundary. Let  $T_1$  and  $T_2$  be two triangulations that contain the upper and  
 202 the lower extreme triangulation of  $D$  as a sub-triangulation, respectively. Let  $\sigma$  be a flip  
 203 sequence from  $T_1$  to  $T_2$  such that there is no triangulation in  $\sigma$  containing a triangle  
 204 with one vertex at the upper chain, the other vertex at the lower chain, and the third  
 205 vertex at a point in the interior of the hourglass of  $D$ . Then  $|\sigma| \geq (h - 1)^2$ .*

206 *Proof* Our reasoning is similar to the proof of Lemma 3.3, see also [18]. As before, let  
 207  $C_u$  and  $C_l$  be the upper and lower chain of  $D$ , and call a triangle with an edge on  $C_u$  or  
 208 on  $C_l$  *anchored*, the third vertex being the *apex*. Any triangulation of the given polygon  
 209 has  $2(h - 1)$  anchored triangles.

210 We will argue that for each triangulation of  $\sigma$  there exists a line  $\ell$  that separates  
 211  $C_u$  from  $C_l$  and that intersects all anchored triangles. This is clear if the apices of  
 212 all anchored triangles lie on the other chain or outside the hourglass. Now consider a  
 213 triangulation of the sequence  $\sigma$  where at least one anchored triangle has its apex at a  
 214 vertex  $v$  inside the hourglass. Let  $r$  be a ray that starts at a point on  $u_0l_0$  and passes  
 215 through  $v$  such that the supporting line of  $r$  separates  $C_u$  from  $C_l$  (such a ray must  
 216 exist since  $v$  is inside the hourglass). Then  $r$  intersects at least one triangle that is not



217 anchored, because the triangle whose interior is intersected by  $r$  before reaching  $v$  cannot  
 218 be anchored. Let  $\Delta$  be the first non-anchored triangle whose interior is intersected by  $r$ .  
 219 Then  $\Delta$  has one vertex on  $C_u$  and one vertex on  $C_l$ . By assumption, the third vertex  
 220 of  $\Delta$  cannot be inside the hourglass, so it must lie outside. This means that one of the  
 221 vertices of  $\Delta$  has to be either  $u_{h-1}$  or  $l_{h-1}$ . This implies that either all anchored triangles  
 222 at  $C_u$  or all anchored triangles  $C_l$ , respectively, have their apex at the opposite chain.  
 223 Thus, also for this triangulation there exists a line  $\ell$  that separates  $C_u$  from  $C_l$  and that  
 224 intersects all anchored triangles. Observe that every such line intersects the anchored  
 225 triangles in the same order.

226 Now we proceed similarly as in the proof of Hurtado, Noy, and Urrutia [11]: we  
 227 observe that an anchored triangle at  $C_u$  and an anchored triangle at  $C_l$  can change their  
 228 relative position along  $\ell$  only if they have an edge in common and this edge is flipped.  
 229 This results in an overall number of  $(h-1)^2$  flips.  $\square$

#### 230 4 The Reduction

231 We reduce YRSA to POLYFLIP. Let  $S$  be a set of  $N$  sinks. By Corollary 2.3, we can  
 232 assume that the coordinates of sinks of  $S$  are multiples of a factor  $\beta = 2N$  in  $\{0, \dots, \beta n\}$ .  
 233 Further, we can restrict ourselves to YRSA instances of the form  $(S, \beta k)$ . Thus, we  
 234 imagine that the sinks are embedded on a  $\beta n \times \beta n$  grid. The reasons for the choice of  $\beta$   
 235 will become clear below.

236 We construct a polygon  $P$  and two triangulations  $T_1, T_2$  in  $P$  such that a shortest  
 237 flip sequence from  $T_1$  to  $T_2$  corresponds to a shortest RSA for  $S$ . To this end, we will  
 238 describe how to interpret any triangulation of  $P$  as a *chain path*, a path in the integer  
 239 grid that starts at the root and uses only edges that go north or east. It will turn out  
 240 that flips in  $P$  essentially correspond to moving the endpoint of the chain path along the  
 241 grid. We choose  $P, T_1$ , and  $T_2$  in such a way that a shortest flip sequence between  $T_1$  and  
 242  $T_2$  moves the endpoint of the chain path according to an Eulerian traversal of a shortest  
 243 RSA for  $S$ . To force the chain path to visit all sinks, we use the observations from  
 244 Section 3: the polygon  $P$  contains a double chain for each sink, so that only for certain  
 245 triangulations of  $P$  it is possible to flip the double chain quickly. These triangulations will  
 246 be exactly the triangulations that correspond to the chain path visiting the appropriate  
 247 sink. To force the sinks to be visited, we, with foresight, fix the number of points in

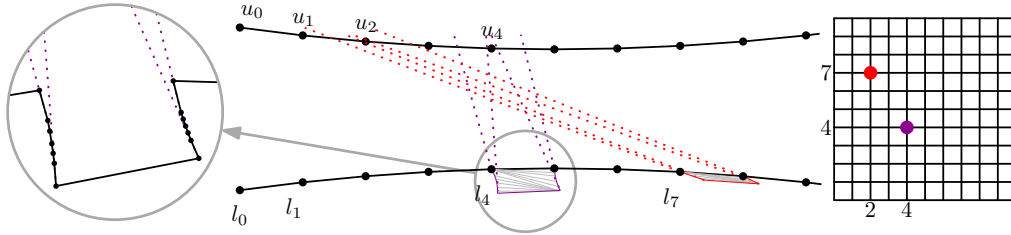


**Fig. 4** The sink gadget for a sink  $(x_s, y_s)$  is obtained by replacing the edge  $l_{y_s}l_{y_s+1}$  by a double chain with  $d$  vertices on each chain. The double chain is oriented such that  $u_{x_s}$  is the only point inside its hourglass and its flip-kernel.

248 each of the two chains of a double chain representing a sink to  $d = nN$  (recall that  $n$  is  
 249 polynomial in  $N$ ).

#### 250 4.1 The Construction

251 We take a double chain  $D$  with  $\beta n + 2$  vertices on each chain such that the flip-kernel  
 252 of  $D$  extends to the right of  $l_{\beta n+1}u_{\beta n+1}$ . We add a point  $z$  to that part of the flip-kernel,  
 253 and we let  $Q$  be the polygon defined by  $\langle l_0, \dots, l_{\beta n+1}, z, u_{\beta n+1}, \dots, u_0 \rangle$ , i.e., a double  
 254 chain extended by  $z$  (recall Definition 3.2). Next, we add double chains to  $Q$  in order  
 255 to encode the sinks in  $S$ . For each sink  $s = (x_s, y_s)$ , we remove the edge  $l_{y_s}l_{y_s+1}$ , and  
 256 we replace it by a (rotated) double chain  $D_s$  with  $d$  vertices on each chain, such that  $l_{y_s}$   
 257 and  $l_{y_s+1}$  become the last point on the lower and the upper chain of  $D_s$ , respectively.  
 258 We orient  $D_s$  in such a way that  $u_{x_s}$  is the only point inside the hourglass of  $D_s$  and so  
 259 that  $u_{x_s}$  lies in the flip-kernel of  $D_s$ ; see Fig. 4. We refer to the added double chains as  
 260 the *sink gadgets*, and we call the resulting polygon  $P$ . Since the  $y$ -coordinates in  $S$  are  
 261 pairwise distinct, there is at most one sink gadget per edge of the lower chain of  $Q$ . Since  
 262  $\beta \geq 2$ , no two sink gadgets are placed on neighboring edges of  $Q$ , and can be constructed  
 263 such that they do not overlap. Hence,  $P$  is a simple polygon. The precise placement of  
 264 the sink gadgets is flexible, so given an appropriate embedding of  $D$ , we can make all  
 265 coordinates integers whose value is polynomial in the input size; see Appendix A for  
 266 details.

267 Next, we describe the source and target triangulation for  $P$ . In the source triangulation  
 268  $T_1$ , the interior of  $Q$  is triangulated such that all edges are incident to  $z$ . The sink  
 269 gadgets are all triangulated with the upper extreme triangulation. The target triangulation

270 tion  $T_2$  is similar, but now the sink gadgets are all triangulated with the lower extreme  
271 triangulation.

272 To get from  $T_1$  to  $T_2$ , we must go from one extreme triangulation to the other for  
273 each sink gadget  $D_s$ . By Lemma 3.4, this requires  $(d-1)^2$  flips, unless the flip sequence  
274 creates a triangle that allows us to use the vertex in the flip-kernel of  $D_s$ . In this case,  
275 we say that the flip sequence *visits* the sink  $s$ . The main idea is that, since the value  
276 chosen for  $d$  is large, a shortest flip sequence must visit all sinks, and we will show that  
277 this induces an RSA for  $S$  of comparable length. Conversely, we will show how to derive  
278 a flip sequence from an RSA. The precise statement is given in the following theorem.

279 **Theorem 4.1** *Let  $N \geq 3$ , and set  $\beta = 2N$ . Let  $S$  be a set of  $N$  sinks such that  
280 the coordinates of the sinks are multiples of  $\beta$  in  $\{0, \dots, \beta n\}$ , where  $n$  is polynomially  
281 bounded in  $N$ . Set  $d = nN$  and let  $P$  be the simple polygon and  $T_1$  and  $T_2$  the two  
282 triangulations of  $P$  as described above. Then for any  $k \geq 1$ , the flip distance between  $T_1$   
283 and  $T_2$  w.r.t.  $P$  is at most  $2\beta k + (4d - 2)N$  if and only if  $S$  has an RSA of length at  
284 most  $\beta k$ .*

285 We will prove Theorem 4.1 in the following sections. But first, let us show how to  
286 use it for our NP-completeness result.

287 **Theorem 4.2** *POLYFLIP is NP-complete.*

288 *Proof* As mentioned in the introduction, the flip distance in polygons is polynomially  
289 bounded, so POLYFLIP is in NP. We reduce from YRSA. Let  $(S, \beta k)$  be an instance of  
290 YRSA as above. We construct  $P$  and  $T_1, T_2$  as described above. This takes polynomial  
291 time (see Appendix A for details on the coordinate representation). By Theorem 4.1,  
292 there exists an RSA for  $S$  of length at most  $\beta k$  if and only if there exists a flip sequence  
293 between  $T_1$  and  $T_2$  of length at most  $2\beta k + (4d - 2)N$ .  $\square$

## 294 4.2 Chain Paths

295 Now we introduce the *chain path*, our main tool to establish a correspondence between  
296 flip sequences and RSAs. Let  $T$  be a triangulation of  $Q$  (i.e., the polygon  $P$  without the  
297 sink gadgets, cf. Section 4.1). A *chain edge* is an edge of  $T$  between the upper and the  
298 lower chain of  $Q$ . A *chain triangle* is a triangle of  $T$  that contains two chain edges. Let  
299  $e_1, \dots, e_m$  be the chain edges, sorted from left to right according to their intersection



323 **Lemma 4.7** *Any triangulation  $T$  of  $Q$  uniquely determines a chain path, and vice versa.*  
 324 *A flip in  $T$  corresponds to one of the following operations on the chain path: (i) move*  
 325 *the endpoint  $b$  north or east; (ii) shorten the path at  $b$ ; (iii) change an east-north bend*  
 326 *to a north-east bend, or vice versa.  $\square$*

### 327 4.3 From an RSA to a Short Flip Sequence

328 Using the notion of a chain path, we now prove the “if” direction of Theorem 4.1.

329 **Lemma 4.8** *Let  $k \geq 1$  and  $A$  an RSA for  $S$  of length  $\beta k$ . Then the flip distance between*  
 330  *$T_1$  and  $T_2$  w.r.t.  $P$  is at most  $2\beta k + (4d - 2)N$ .*

331 *Proof* The triangulations  $T_1$  and  $T_2$  both contain a triangulation of  $Q$  whose chain path  
 332 has its endpoint  $b$  at the root. We use Lemma 4.7 to generate flips inside  $Q$  so that  $b$   
 333 traverses  $A$  in a depth-first manner. This needs  $2\beta k$  flips.

334 Each time  $b$  reaches a sink  $s$ , we move  $b$  north. This creates a chain triangle that  
 335 allows the edges in the sink gadget  $D_s$  to be flipped to the auxiliary vertex in the  
 336 flip-kernel of  $D_s$ . The triangulation of  $D_s$  can then be changed with  $4d - 4$  flips; see  
 337 Lemma 3.3. Next, we move  $b$  back south and continue the traversal. Moving  $b$  at  $s$  needs  
 338 two additional flips, so we take  $4d - 2$  flips per sink, for a total of  $2\beta k + (4d - 2)N$   
 339 flips.  $\square$

### 340 4.4 From a Short Flip Sequence to an RSA

341 Finally, we consider the “only if” direction in Theorem 4.1. Let  $\tau$  be a flip sequence on  $Q$ .  
 342 We say that  $\tau$  *visits* a sink  $s = (x_s, y_s)$  if  $\tau$  has at least one triangulation that contains  
 343 the chain triangle  $u_{x_s} l_{y_s} l_{y_s+1}$ . We call  $\tau$  a *flip traversal* for  $S$  if (i)  $\tau$  begins and ends  
 344 in the triangulation whose corresponding chain path has its endpoint  $b$  at the root and  
 345 (ii)  $\tau$  visits every sink in  $S$ . The following lemma shows that every short flip sequence  $\sigma$   
 346 in  $P$  can be mapped to a flip traversal (where with “short”, we mean  $|\sigma| < (d - 1)^2$ ).

347 **Lemma 4.9** *Let  $\sigma$  be a flip sequence from  $T_1$  to  $T_2$  w.r.t.  $P$  with  $|\sigma| < (d - 1)^2$ . Then*  
 348 *there is a flip traversal  $\tau$  for  $S$  with  $|\tau| \leq |\sigma| - (4d - 4)N$ .*

349 *Proof* We show how to obtain a flip traversal  $\tau$  for  $S$  from  $\sigma$ . Let  $T$  be a triangulation  
 350 of  $P$ . A triangle of  $T$  is an *inner triangle* if all its sides are diagonals. It is an *ear* if two

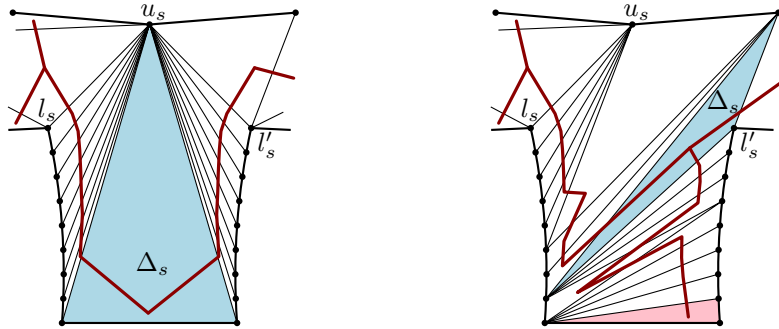


**Fig. 6** Triangulations of  $D_s$  in  $P$  with  $\Delta_s = \Delta$  (left), and with  $\Delta$  being an ear (red) and  $\Delta_s$  an inner triangle (right). The fat tree indicates the dual.

351 of its sides are polygon edges. By construction, every inner triangle of  $T$  must have (i)  
 352 one vertex incident to  $z$  (the rightmost vertex of  $Q$ ), or (ii) two vertices incident to a  
 353 sink gadget (or both). There can be only one triangle of type (ii) per sink gadget. The  
 354 weak (graph theoretic) dual of  $T$  is a tree in which ears correspond to leaves and inner  
 355 triangles have degree 3.

356 For a sink  $s = (x_s, y_s)$ , let  $D_s$  be the corresponding sink gadget. It lies between  
 357 the vertices  $l_{y_s}$  and  $l_{y_s+1}$  and has exactly  $u_{x_s}$  in its flip kernel. For brevity, we will  
 358 write  $l_s$  for  $l_{y_s}$ ,  $l'_s$  for  $l_{y_s+1}$ , and  $u_s$  for  $u_{x_s}$ . We define a triangle  $\Delta_s$  for  $D_s$ . Consider  
 359 the bottommost edge  $e$  of  $D_s$ , and let  $\Delta$  be the triangle of  $T$  that is incident to  $e$ . By  
 360 construction,  $\Delta$  is either an ear of  $T$ , or it is the triangle defined by  $e$  and  $u_s$ . In the  
 361 latter case, we set  $\Delta_s = \Delta$ . In the former case, we claim that  $T$  has an inner triangle  
 362  $\Delta'$  with two vertices on  $D_s$ : follow the path from  $\Delta$  in the weak dual of  $T$ ; while the  
 363 path does not encounter an inner triangle, the next triangle must have an edge of  $D_s$   
 364 as a side. There is only a limited number of such edges, so eventually we must meet an  
 365 inner triangle  $\Delta'$ . We then set  $\Delta_s = \Delta'$ ; see Fig. 6. Note that  $\Delta_s$  might be  $l_s l'_s u_s$ .

366 For each sink  $s$ , let the polygon  $Q_s$  consist of  $D_s$  extended by the vertex  $u_s$  (cf. Def-  
 367 inition 3.2). Let  $T$  be a triangulation of  $P$ . We show how to map  $T$  to a triangulation  
 368  $T_Q$  of  $Q$  and to triangulations  $T_s$  of  $Q_s$ , for each  $s$ .

369 We first describe  $T_Q$ . It contains every triangle of  $T$  with all three vertices in  $Q$ . For  
 370 each triangle  $\Delta$  in  $T$  with two vertices on  $Q$  and one vertex on the left chain of a sink  
 371 gadget  $D_s$ , we replace the vertex on  $D_s$  by  $l_s$ . Similarly, if the third vertex of  $\Delta$  is on the  
 372 right chain of  $D_s$ , we replace it by  $l'_s$ . For every sink  $s$ , the triangle  $\Delta_s$  has one vertex

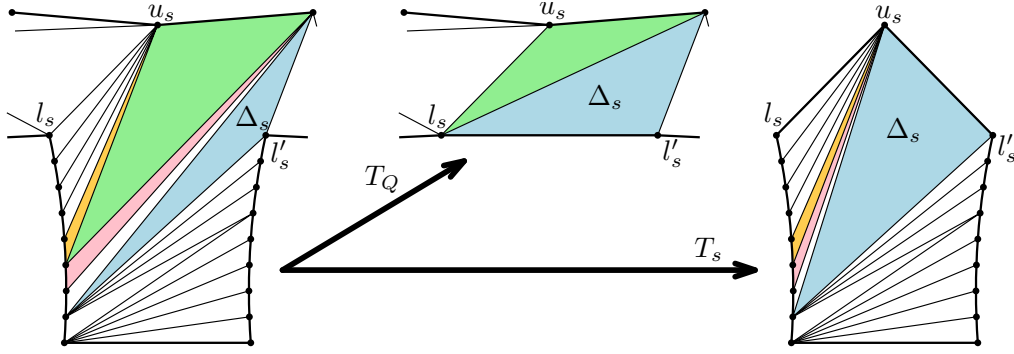


Fig. 7 Obtaining  $T_Q$  and  $T_s$  from  $T$ .

373 at a point  $u_i$  of the upper chain. In  $T_Q$ , we replace  $\Delta_s$  by the triangle  $l_s l'_s u_i$ . No two  
 374 triangles in  $T_Q$  overlap, and they cover all of  $Q$ . Thus,  $T_Q$  is indeed a triangulation of  $Q$ .

375 Now we describe how to obtain  $T_s$ , for a sink  $s \in S$ . Each triangle of  $T$  with all  
 376 vertices on  $Q_s$  is also in  $T_s$ . Each triangle with two vertices on  $D_s$  and one vertex not  
 377 in  $Q_s$  is replaced in  $T_s$  by a triangle whose third vertex is moved to  $u_s$  in  $T_s$  (note that  
 378 this includes  $\Delta_s$ ); see Fig. 7. Again, all triangles cover  $Q_s$  and no two triangles overlap.

379 Finally, we show that a flip in  $T$  corresponds to at most one flip either in  $T_Q$  or in  
 380 precisely one  $T_s$  for some sink  $s$ . We do this by considering all the possibilities for two  
 381 triangles that share a common flippable edge. By construction, no two triangles that are  
 382 mapped to two different triangulations  $T_s$  and  $T_t$  for sinks  $s \neq t \in S$  can share an edge.

383 **Case 1.** We flip an edge between two triangles that are either both mapped to  $T_Q$  or  
 384 to  $T_s$  and are different from  $\Delta_s$ . This flip clearly happens in at most one triangulation.

385 **Case 2.** We flip an edge between a triangle  $\Delta_1$  that is mapped to  $T_s$  and a triangle  $\Delta_2$   
 386 that is mapped to  $T_Q$ , such that both  $\Delta_1$  and  $\Delta_2$  are different from  $\Delta_s$ . This results in  
 387 a triangle  $\Delta'_1$  that is incident to the same edge of  $Q_s$  as  $\Delta_1$ , and a triangle  $\Delta'_2$  having  
 388 the same vertices of  $Q$  as  $\Delta_2$ . Since the apex of  $\Delta_1$  is a vertex of the upper chain or  $z$   
 389 (otherwise, it would not share an edge with  $\Delta_2$ ), it is mapped to  $u_s$ , as is the apex of  $\Delta'_1$ .  
 390 Also, the apex of  $\Delta'_2$  is on the same chain of  $D_s$  as the one of  $\Delta_2$ . Hence, the flip affects  
 391 neither  $T_Q$  nor  $T_s$ .

392 **Case 3.** We flip the edge between a triangle  $\Delta_2$  mapped to  $T_Q$  and  $\Delta_s$ . By construc-  
 393 tion, this can only happen if  $\Delta_s$  is an inner triangle. The flip affects only  $T_Q$ , because  
 394 the new inner triangle  $\Delta'_s$  is mapped to the same triangle in  $T_s$  as  $\Delta_s$ , since both apexes  
 395 are moved to  $u_s$ .

396 **Case 4.** We flip the edge between a triangle  $\Delta$  of  $T_s$  and  $\Delta_s$ . Similar to Case 3,  
 397 this affects only  $T_s$ , because the new triangle  $\Delta'_s$  is mapped to the same triangle in  $T_Q$   
 398 as  $\Delta_s$ , since the two corners are always mapped to  $l_s$  and  $l'_s$ .

399 Thus,  $\sigma$  induces a flip sequence  $\tau$  in  $Q$  and flip sequences  $\sigma_s$  in each  $Q_s$  so that  
 400  $|\tau| + \sum_{s \in S} |\sigma_s| \leq |\sigma|$ . Furthermore, each flip sequence  $\sigma_s$  transforms  $Q_s$  from one ex-  
 401 tremite triangulation to the other. Since  $|\sigma| < (d-1)^2$ , Lemma 3.4 tells us that the  
 402 triangulations  $T_s$  have to be transformed so that  $\Delta_s$  has a vertex at  $u_s$  at some point.  
 403 Moreover, by Lemma 3.3, we have  $|\sigma_s| \geq 4d-4$  for each  $s \in S$ . Thus,  $\tau$  is a flip traversal,  
 404 and  $|\tau| \leq |\sigma| - N(4d-4)$ , as claimed.  $\square$

405 In order to obtain a static RSA from a changing flip traversal, we use the notion  
 406 of a *trace*. A *trace* is a domain on the grid. It consists of *edges* and *boxes*: an edge is  
 407 a line segment of length 1 whose endpoints have positive integer coordinates; a box is  
 408 a square of side length 1 whose corners have positive integer coordinates. Similar to  
 409 arborescences, we require that a trace  $R$  (i) is (topologically) connected; (ii) contains  
 410 the root  $(0,0)$ ; and (iii) from every grid point contained in  $R$  there exists an  $x$ - and  
 411  $y$ -monotone path to the root that lies completely in  $R$ . We say  $R$  is a *covering trace*  
 412 for  $S$  (or,  $R$  *covers*  $S$ ) if every sink in  $S$  is covered by  $R$  (i.e., incident to a box or an  
 413 edge in  $R$ ).

414 Let  $\tau$  be a flip traversal as in Lemma 4.9. By Lemma 4.7, each triangulation in  $\tau$   
 415 corresponds to a chain path. This gives a covering trace  $R$  for  $S$  in the following way.  
 416 For every flip in  $\tau$  that extends the chain path, we add the corresponding edge to  $R$ .  
 417 For every flip in  $\tau$  that changes a bend, we add the corresponding box to  $R$ . Afterwards,  
 418 we remove from  $R$  all edges that coincide with a side of a box in  $R$ . Clearly,  $R$  is  
 419 (topologically) connected. Since  $\tau$  is a flip traversal for  $S$ , every sink is covered by  $R$ .  
 420 Note that every grid point  $p$  in  $R$  is connected to the root by an  $x$ - and  $y$ -monotone  
 421 path on  $R$ , since at some point  $p$  belonged to a chain path in  $\tau$ . Hence,  $R$  is indeed a  
 422 trace, the unique *trace of*  $\tau$ . Note that not only a flip traversal but any flip sequence  
 423 starting with a zero-length chain path defines a trace in this way.

424 Next, we define the *cost* of a trace  $R$ ,  $\text{cost}(R)$ , so that if  $R$  is the trace of a flip  
 425 traversal  $\tau$ , then  $\text{cost}(R)$  gives a lower bound on  $|\tau|$ . An edge has cost 2. Let  $B$  be a box  
 426 in  $R$ . A *boundary side* of  $B$  is a side that is not part of another box. The cost of  $B$  is 1  
 427 plus the number of boundary sides of  $B$ . Then,  $\text{cost}(R)$  is the total cost over all boxes



428 and edges in  $R$ . For example, the cost of a tree is twice the number of its edges, and  
 429 the cost of a rectangle is its area plus its perimeter. An edge can be interpreted as a  
 430 degenerated box, having two boundary sides and no interior.

431 **Proposition 4.10** *Let  $\tau$  be a flip traversal and  $R$  the trace of  $\tau$ . Then  $\text{cost}(R) \leq |\tau|$ .*

432 *Proof* Let  $\varsigma_i$  be the sequence of the first  $i$  triangulations of  $\tau$ ,  $R_i$  the trace defined by  $\varsigma_i$ ,  
 433 and let  $\kappa_i$  be the length of the chain path for the  $i$ th triangulation. We will show by  
 434 induction on  $i$  that  $\text{cost}(R_i) \leq i + \kappa_i$ , for  $i = 1, \dots, |\tau|$ . Since  $\varsigma_{|\tau|} = \tau$ ,  $R_{|\tau|} = R$ , and  
 435  $\kappa_{|\tau|} = 0$ , this gives the desired result.

436 After the first flip,  $R_1$  is an edge (so  $\text{cost}(R_1) = 2$ ), and  $\kappa_1 = 1$ , which fulfills the  
 437 invariant. Consider the  $i$ th flip. If the flip extends the chain path, the cost of the trace  
 438 increases by at most 2, and the length of the chain path increases by 1, fulfilling the  
 439 invariant. If the flip contracts the chain path, the trace does not change, but the length  
 440 of the chain path is decreased by 1, again fulfilling the invariant. We are therefore left  
 441 with the case where the flip is a chain flip. We have  $\kappa_{i-1} = \kappa_i$ , so we have to show  
 442 that  $\text{cost}(R_i) \leq \text{cost}(R_{i-1}) + 1$ . We may assume that the flip adds a box  $B$  to  $R_{i-1}$   
 443 (otherwise, the cost of the trace remains unchanged). Consider the intersection of the  
 444 boundary of  $B$  with the one of  $R_{i-1}$ . This intersection contains at least two elements,  
 445 as the chain path is part of  $R_{i-1}$ . An edge in the intersection becomes a boundary side  
 446 in  $R_i$ , reducing the cost by 1. A boundary side in the intersection vanishes in  $R_i$ , also  
 447 reducing the cost by 1. Thus, adding  $B$  creates a box and at most two boundary sides,  
 448 causing a cost of at most 3, but it simultaneously reduces the cost by at least 2. See  
 449 the examples in Fig. 8. The overall cost increases at most by 1, and the invariant is  
 450 maintained.  $\square$

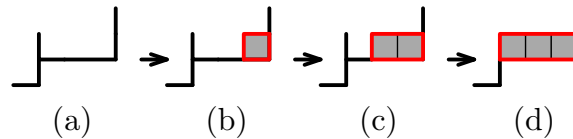


**Fig. 8** Examples of how boundary sides (red) are added to a trace. To a trace of cost 16 (a) a box (gray) is added (b), which transforms two edges in boundary sides and adds two boundary sides, resulting in an overall cost of 17. The next box removes one boundary side and one edge and adds three boundary sides (c), the cost becomes 18. A box might also remove more than two elements (d), reducing the overall cost to 17.

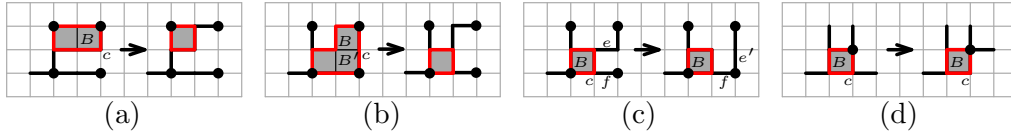


**Fig. 9** Parts of traces to be modified; the boundary sides are shown in red. (a) A box that has a corner  $c$  with no incident elements can be removed. (b) Two adjacent boxes that have a shared corner  $c$  without any incident elements can be removed. (c) Replacing a single edge. (d) Sliding an edge.

451 Now we relate the length of an RSA for  $S$  to the cost of a covering trace for  $S$ , and  
 452 thus to the length of a flip traversal. Since each sink is connected in  $R$  to the root by an  
 453  $x$ - and  $y$ -monotone path, traces can be regarded as generalized RSAs. In particular, we  
 454 make the following observation.

455 **Observation 4.11** *Let  $R$  be a covering trace for  $S$  that contains no boxes, and let  $A_\tau$*   
 456 *be a shortest path tree in  $R$  from the root to all sinks in  $S$ . Then  $A_\tau$  is an RSA for  $S$ .  $\square$*

457 If  $\tau$  contains no flips that change bends, the corresponding trace  $R$  has no boxes.  
 458 Then,  $R$  contains an RSA  $A_\tau$  with  $2|A_\tau| \leq \text{cost}(R)$ , by Observation 4.11. The next  
 459 lemma shows that, due to the fact that  $\beta$  is even, there is always a shortest covering  
 460 trace for  $S$  that does not contain any boxes.

461 **Lemma 4.12** *Let  $\tau$  be a flip traversal of  $S$ . Then there exists a covering trace  $R$  for  $S$*   
 462 *such that  $R$  does not contain a box and such that  $\text{cost}(R) \leq |\tau|$ .*

463 To prove the lemma, we investigate the structure of minimal covering traces. There  
 464 exists at least one trace of cost at most  $|\tau|$ , namely the trace of  $\tau$ . Let  $\mathcal{R}_1$  be the set of  
 465 all covering traces for  $S$  that have minimum cost. Let  $\mathcal{R}_2 \subseteq \mathcal{R}_1$  be those covering traces  
 466 among  $\mathcal{R}_1$  that contain the minimum number of boxes. If  $\mathcal{R}_2$  contains a trace without  
 467 boxes, we are done, as every covering trace in  $\mathcal{R}_2$  fulfills the requirements of Lemma 4.12.  
 468 We show that this is actually the case by assuming, for the sake of contradiction, that  
 469 every covering trace in  $\mathcal{R}_2$  contains at least one box.

470 Let  $R \in \mathcal{R}_2$  and suppose that  $R$  contains a box. Let  $B$  be a *maximal* box in  $R$ , i.e.,  $R$   
 471 has no other box whose lower left corner has both  $x$ - and  $y$ -coordinate at least as large  
 472 as the lower left corner of  $B$ . In order to prove Lemma 4.12, we need several lemmata  
 473 on traces of minimum cost.

474 **Lemma 4.13** *Let  $B$  be a maximal box and let  $c$  a corner of  $B$  that is not the root  $(0, 0)$ .*  
 475 *Then  $c$  is incident either to a sink, an edge, or another box.*

476 *Proof* Suppose there exists a corner  $c$  for which this is not the case. Note that such a  $c$   
 477 cannot be the lower left corner of  $B$ , as there has to be an  $x$ - and  $y$ -monotone path to  
 478 the root. Hence, we could remove  $c$  and  $B$  while keeping the sides of  $B$  not incident to  $c$   
 479 as edges, if necessary; see Fig. 9(a). In the resulting structure, every element still has  
 480 an  $x$ - and  $y$ -monotone path to the root: If  $c$  is the lower right or upper left corner, any  
 481 path initially passing through  $c$  could be rerouted to pass through the corner opposite  
 482 of  $c$  in  $B$ . If  $c$  is the upper right corner of  $B$ , no path is passing through  $c$ . Hence, the  
 483 resulting structure would be a covering trace with smaller cost, contradicting the choice  
 484 of  $R$ .  $\square$

485 **Lemma 4.14** *Suppose  $B$  shares a horizontal side with another box  $B'$ . Let  $c$  be the right*  
 486 *endpoint of the common side. Then  $c$  is incident either to a sink, an edge, or another*  
 487 *box.*

488 *Proof* Suppose this is not the case. Then we could remove  $B$  and  $B'$  from  $R$  while  
 489 keeping the sides not incident to  $c$  as edges, if necessary; see Fig. 9(b). This results in  
 490 a valid trace that has no higher cost but less boxes than  $R$ , contradicting the choice  
 491 of  $R$ .  $\square$

492 **Lemma 4.15** *Let  $c$  be the lower right corner of  $B$ . Then  $c$  has no incident vertical edge.*

493 *Proof* Such an edge would be redundant, since  $c$  already has an  $x$ - and  $y$ -monotone path  
 494 to the root that goes through the lower left corner of  $B$ .  $\square$

495 *Proof (Proof of Lemma 4.12)* Using the Lemmata 4.13, 4.14, and 4.15, we derive a  
 496 contradiction from the choice of  $R$  and the maximal box  $B$ . Note that since  $\beta$  is even,  
 497 all sinks in  $S$  have even  $x$ - and  $y$ -coordinates. We distinguish two cases.

498 **Case 1.** There exists a maximal box  $B$  whose top right corner  $c'$  does not have both  
 499 coordinates even. Suppose that the  $x$ -coordinate of  $c'$  is odd. (Otherwise, mirror the  
 500 plane at the line  $x = y$  to swap the  $x$ - and the  $y$ -axis. Note that the property of being  
 501 a trace is invariant under mirroring the plane along the line  $x = y$ ; in particular, the  
 502 choice of  $B$  in  $R$  as a maximal box remains valid) By Lemma 4.13, there is at least  
 503 one edge incident to the top right corner of  $B$  (it cannot be a box by the choice of  $B$ ,  
 504 and it cannot be a sink because of the current case). Recall the slide operation for an  
 505 edge in an arborescence. This operation can easily be adapted in an analogous way to  
 506 traces. If there is a vertical edge  $v$  incident to  $c'$ , it cannot be incident to a sink. Thus,

507 we could slide  $v$  to the right (together with all other vertical edges that are above  $v$   
 508 and on the supporting line of  $v$ ). Hence, we may assume that  $c'$  is incident to a single  
 509 horizontal edge  $e$ ; see Fig. 9(c). By Lemma 4.13, the bottom right corner  $c$  of  $B$  must be  
 510 incident to an element. We know that  $c$  cannot be the top right corner of another box  
 511 (Lemma 4.14), nor can it be incident to a vertical segment (Lemma 4.15). Thus,  $c$  is  
 512 incident to an element  $f$  that is either a horizontal edge or a box with top left corner  $c$ .  
 513 But then  $e$  could be replaced by a vertical segment  $e'$  incident to  $f$ , and afterwards  $B$   
 514 could be removed as in the proof of Lemma 4.13, contradicting the choice of  $R$ .

515 **Case 2.** The top right corner of each maximal box has even coordinates. Let  $B$  be  
 516 the rightmost maximal box. As before, let  $c$  be the bottom right corner of  $B$ . The  $y$ -  
 517 coordinate of  $c$  is odd; see Fig. 9(d). By the choice of  $B$ , we know that  $c$  is not the  
 518 top left corner of another box: this would imply that there is another maximal box to  
 519 the right of  $B$ . We may assume that  $c$  is not incident to a horizontal edge, as we could  
 520 slide such an edge up, as in Case 1. Furthermore,  $c$  cannot be incident to a vertical  
 521 edge (Lemma 4.15), nor be the top right corner of another box (Lemma 4.14). Thus,  $B$   
 522 violates Lemma 4.13, and Case 2 also leads to a contradiction.

523 Thus, the choice of  $R$  forces a contradiction in either case. Hence, the minimum  
 524 number of boxes in a minimum covering trace for  $S$  is 0.  $\square$

525 Now we can finally complete the proof of Theorem 4.1 by giving the second direction of  
 526 the correspondence.

527 **Lemma 4.16** *Let  $k \geq 1$  and let  $\sigma$  be a flip sequence on  $P$  from  $T_1$  to  $T_2$  with  $|\sigma| \leq$   
 528  $2\beta k + (4d - 2)N$ . Then there exists an RSA for  $S$  of length at most  $\beta k$ .*

529 *Proof* Trivially, there always exists an RSA on  $S$  of length less than  $2\beta nN$ , so we may  
 530 assume that  $k < 2nN$ . Hence (recall that  $\beta = 2N$  and  $d = nN$ ),

$$531 \quad 2\beta k + (4d - 2)N < 2 \cdot 2N \cdot 2nN + 4nN^2 - 2N < 12nN^2 < (d - 1)^2,$$

532 for  $n \geq 14$  and positive  $N$ . Thus,  $\sigma$  meets the requirements of Lemma 4.9, and therefore  
 533 we can obtain a flip traversal  $\tau$  for  $S$  with  $|\tau| \leq 2\beta k + 2N$ . By Lemma 4.12 and  
 534 Observation 4.11, we can conclude that there is an RSA  $A$  for  $S$  that has length at most  
 535  $\beta k + N$ . By Theorem 2.1, there is an RSA  $A'$  for  $S$  that is not longer than  $A$  and that  
 536 lies on the Hanan grid for  $S$ . The length of  $A'$  must be a multiple of  $\beta$ . Thus, since  
 537  $\beta > N$ , we get that  $A'$  has length at most  $\beta k$ .  $\square$

## 538 5 Conclusion

539 In this paper, we showed NP-hardness of determining a shortest flip sequence between  
540 two triangulations of a simple polygon. This complements the recent hardness results  
541 for point sets (obtained by reduction from variants of VERTEX COVER). However, while  
542 for point sets the problem is hard to approximate as well, our reduction does not rule  
543 out the existence of a polynomial-time approximation scheme (PTAS), since a PTAS  
544 is known for the RSA problem [17]. When problems that are hard for point sets are  
545 restricted to simple polygons, the application of standard techniques—like dynamic  
546 programming—often gives polynomial-time algorithms. This is, for example, the case  
547 for the construction of the minimum weight triangulation. Our result illustrates that de-  
548 termining the flip distance is a different, harder type of problem. Is there a PTAS for the  
549 flip distance between triangulations of a polygon? Even a constant-factor approximation  
550 would be interesting.

551 For convex polygons (or, equivalently, points in convex position), the complexity  
552 of the problem remains unknown. Our construction heavily relies on the double chain  
553 construction, using many reflex vertices. Does the problem remain hard if we restrict  
554 the number of reflex vertices to some constant fraction?

## 555 References

- 556 1. Abel, Z., Ballinger, B., Bose, P., Collette, S., Dujmović, V., Hurtado, F., Kominers, S., Langerman,  
557 S., Pór, A., Wood, D.: Every large point set contains many collinear points or an empty pentagon.  
558 *Graphs Combin.* **27**, 47–60 (2011)
- 559 2. Aichholzer, O., Mulzer, W., Pilz, A.: Flip Distance Between Triangulations of a Simple Polygon  
560 is NP-Complete. In: Proc. 29<sup>th</sup> European Workshop on Computational Geometry, pp. 115–118.  
561 Braunschweig, Germany (2013)
- 562 3. Aichholzer, O., Mulzer, W., Pilz, A.: Flip distance between triangulations of a simple polygon is  
563 NP-complete. In: H.L. Bodlaender, G.F. Italiano (eds.) *Algorithms - ESA 2013 - 21st Annual*  
564 *European Symposium*, Sophia Antipolis, France, September 2-4, 2013. Proceedings, *Lecture Notes*  
565 *in Computer Science*, vol. 8125, pp. 13–24. Springer (2013)
- 566 4. Bose, P., Hurtado, F.: Flips in planar graphs. *Comput. Geom.* **42**(1), 60–80 (2009)
- 567 5. Canny, J.F., Donald, B.R., Ressler, E.K.: A rational rotation method for robust geometric algo-  
568 rithms. In: Proc. 8<sup>th</sup> Symposium on Computational Geometry (SoCG 1992), pp. 251–260 (1992)
- 569 6. Chazelle, B., Guibas, L.J., Lee, D.T.: The power of geometric duality. *BIT* **25**(1), 76–90 (1985)
- 570 7. Culik II, K., Wood, D.: A note on some tree similarity measures. *Inf. Process. Lett.* **15**(1), 39–42  
571 (1982)

- 
- 572 8. Edelsbrunner, H., O'Rourke, J., Seidel, R.: Constructing arrangements of lines and hyperplanes  
573 with applications. *SIAM J. Comput.* **15**(2), 341–363 (1986)
- 574 9. Eppstein, D.: Happy endings for flip graphs. *JoCG* **1**(1), 3–28 (2010)
- 575 10. Hanke, S., Ottmann, T., Schuierer, S.: The edge-flipping distance of triangulations. *J.UCS* **2**(8),  
576 570–579 (1996)
- 577 11. Hurtado, F., Noy, M., Urrutia, J.: Flipping edges in triangulations. *Discrete Comput. Geom.* **22**,  
578 333–346 (1999)
- 579 12. Husemöller, D.: *Elliptic Curves*. Graduate Texts in Mathematics. Springer-Verlag, New York, NY,  
580 USA (2003)
- 581 13. Hwang, F., Richards, D., Winter, P.: *The Steiner Tree Problem*. Annals of Discrete Mathematics.  
582 North-Holland (1992)
- 583 14. Kanj, I.A., Xia, G.: Flip distance is in FPT time  $O(n + k \cdot c^k)$ . In: 32nd International Symposium  
584 on Theoretical Aspects of Computer Science, STACS, pp. 500–512 (2015)
- 585 15. Lawson, C.L.: Transforming triangulations. *Discrete Math.* **3**(4), 365–372 (1972)
- 586 16. Lawson, C.L.: Software for  $C^1$  surface interpolation. In: J.R. Rice (ed.) *Mathematical Software III*,  
587 pp. 161–194. Academic Press, NY (1977)
- 588 17. Lu, B., Ruan, L.: Polynomial time approximation scheme for the rectilinear Steiner arborescence  
589 problem. *J. Comb. Optim.* **4**(3), 357–363 (2000)
- 590 18. Lubiw, A., Pathak, V.: Flip distance between two triangulations of a point-set is NP-complete. In:  
591 *Proc. 24<sup>th</sup> CCCG*, pp. 127–132 (2012)
- 592 19. Pilz, A.: Flip distance between triangulations of a planar point set is APX-hard. *Comput. Geom.*  
593 **47**(5), 589–604 (2014)
- 594 20. Rao, S.K., Sadayappan, P., Hwang, F.K., Shor, P.W.: The rectilinear Steiner arborescence problem.  
595 *Algorithmica* **7**, 277–288 (1992)
- 596 21. Shi, W., Su, C.: The rectilinear Steiner arborescence problem is NP-complete. In: *Proc. 11<sup>th</sup> SODA*,  
597 pp. 780–787 (2000)
- 598 22. Sleator, D., Tarjan, R., Thurston, W.: Rotation distance, triangulations and hyperbolic geometry.  
599 *J. Amer. Math. Soc.* **1**, 647–682 (1988)
- 600 23. Trubin, V.: Subclass of the Steiner problems on a plane with rectilinear metric. *Cybernetics* **21**,  
601 320–324 (1985)
- 602 24. Urrutia, J.: Algunos problemas abiertos. In: *Proc. IX Encuentros de Geometría Computacional*,  
603 pp. 13–24 (2001)

## 604 A A Note on Coordinate Representation

605 Since it is necessary for the validity of the proof that the input polygon can be represented in size  
 606 polynomial in the size of the YRSA instance, we give a possible method to embed the polygon with  
 607 vertices at rational coordinates whose numerator and denominator are polynomial in  $N$ . By an additional  
 608 perturbation argument we can guarantee integer coordinates whose values are polynomial in  $N$  (which  
 609 slightly strengthens the result). We first introduce the general technique used for the embedding, and  
 610 then give further details on how the sink gadgets are constructed (using methods similar to [19]). Finally,  
 611 we explain how the construction can be transformed to integer points in general position.

### 612 A.1 Placing Points on Arcs

613 The main idea of the construction is to place all vertices on rational points on circular arcs. There are  
 614 two large arcs where we place the vertices of the upper and the lower chain, and smaller arcs on which  
 615 we place the vertices of the sink gadgets. All these circular arcs are chosen from *rational circles*, i.e.,  
 616 circles that are defined by three rational points. Similarly, a *rational line* is a line through a rational  
 617 point with rational slope (or, equivalently, a line defined by two rational points). It is well-known that,  
 618 if one of the two intersection points of a rational line with a rational circle is a rational point, then the  
 619 other intersection point is rational as well (see, e.g., [12, p. 5]). Hence, given a rational point  $p$  on a  
 620 rational circle, we can obtain an arbitrary number of rational points on the circle via different rational  
 621 lines through  $p$ .

622 Let us apply this for one possible way of constructing the double chain  $D$ . The construction is shown  
 623 in Fig. 10 (left). We place the  $\beta n + 2$  points of the lower chain on the unit circle (with center at the  
 624 origin). Let  $\ell_i$  be the line through  $(-1, 0)$  with slope  $1 + \frac{i}{\beta n + 2}$ . For  $i = 1, \dots, \beta n / 2 + 1$ , we get  $\beta n / 2 + 1$   
 625 rational points on the upper-left quadrant of the unit circle from the intersections with this family of  
 626 lines. We can do the analogous construction for points on the upper-right quadrant by choosing lines  
 627 through  $(1, 0)$  with a negative slope  $(-1) - \frac{i}{\beta n + 2}$ . In this way, we obtain the vertices of the lower chain  
 628 of  $D$ . For the upper chain, we place points on the unit circle with origin  $(0, 3)$  analogously. Note that  
 629 line  $\ell_{\beta n / 2 + 1}$  passes through  $(1, 3)$ , so when picking rational points on the lower-right and lower-left  
 630 quadrant of the second unit circle for the upper chain, the resulting point set is indeed the vertex set of  
 631 a double chain in which the line through  $l_0$  and  $u_{\beta n + 1}$  is  $\ell_{\beta n / 2 + 1}$ . Finally, note that all slopes used in  
 632 the construction have numerators and denominators that are polynomial in  $N$ . Hence, this also holds  
 633 for the coordinates of the vertices of  $D$ . Note that this is, essentially, the parametrization of the unit  
 634 circle, as discussed in [5].

635 Clearly, this method is not restricted to unit circles. We now discuss the following main building  
 636 block for constructing the sink gadgets. Given three rational points  $p_1, p_2, p_3$ , we construct a circular  
 637 arc on a rational circle that starts at  $p_1$ , ends at  $p_2$  and is completely contained inside the triangle  
 638  $p_1 p_2 p_3$ . Then, we choose an arbitrary number of rational points on that circular arc. This is illustrated  
 639 in Fig. 10 (right). W.l.o.g, let the inner angle of the triangle at  $p_1$  be less than or equal to the one  
 640 at  $p_2$ . Let  $Z$  be the circle through  $p_1$  and  $p_2$  such that the line  $p_1 p_3$  is a tangent of  $Z$ . Clearly,  $Z$  is  
 641 well-defined, and the arc between  $p_1$  and  $p_2$  is inside the triangle. The circle  $Z$  is rational. (Consider

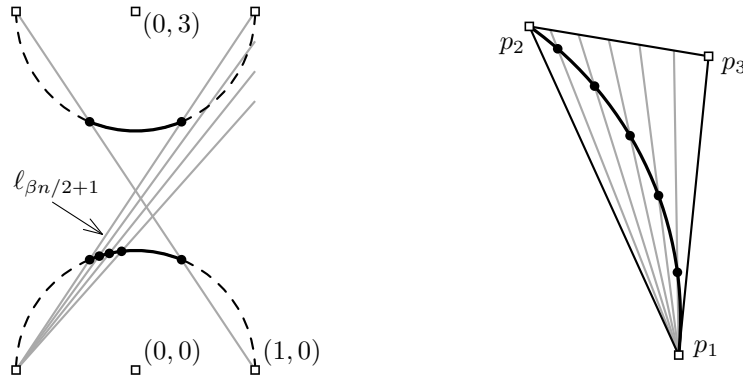


**Fig. 10** Left: Construction of the main double chain  $D$ . Right: Picking points on a circular arc inside a triangle. The line  $p_1p_3$  is tangent to the corresponding circle.

642 the line that is perpendicular to the line  $p_1p_3$  and passes through  $p_1$ . When mirroring  $p_2$  with that  
 643 line as an axis, the resulting point  $p'_2$  is rational and also on  $Z$ .) We can now choose any number of  
 644 rational points on the circular arc by selecting a family of lines through  $p_1$ . To this end, we choose a set  
 645 of equidistant points on the segment  $p_2p_3$ , which, together with  $p_1$  define this family of rational lines.  
 646 Again, the numerators and the denominators are polynomial in those of  $p_1$ ,  $p_2$ , and  $p_3$ , and the number  
 647 of points chosen.

## 648 A.2 Constructing Sink Gadgets

649 We now construct the sink gadgets. See Fig. 11 for an accompanying illustration. Recall that, since  $\beta$  is  
 650 even, there are no small double chains on neighboring positions on the lower chain. Hence, for each sink  
 651 we w.l.o.g. can define an orthogonal region within which we can safely draw the small double chain; we  
 652 call this region the *bin* of the sink (outlined gray in Fig. 11). Consider a sink  $(i, j)$ . The vertical line  
 653 bounding the left side of its bin passes through the edge  $l_{j-1}l_j$  (e.g., at the midpoint of the edge), and  
 654 the right side of the bin is defined analogously. (Recall that, since  $\beta > 1$ , there is no sink at  $l_{j-1}l_j$ .)  
 655 Pick a rational point  $p_a$  on the boundary of the bin that is to the left of the directed line  $l_ju_{i-1}$  and to  
 656 the right of the directed line  $l_ju_i$ . Similarly, choose a point  $p_b$  that is to the right of the line  $l_{j+1}u_{i+1}$   
 657 and to the left of the line  $l_{j+1}u_i$ . As an additional constraint let  $p_a$  be to the left of the line  $p_bu_i$ . Note  
 658 that such points always exist, and can be easily chosen along the boundary of the bin. It remains to  
 659 choose a triangular region with  $l_jp_a$  as one side in which we can place the chain of the sink gadget that  
 660 contains  $l_j$ . For the second chain, the construction is analogous.

661 For the chain to be visible from  $u_i$  but not from  $u_{i-1}$ , the triangular region has to be to the left  
 662 of the line  $p_a u_i$ , and also to the left of the line  $l_j u_{i-1}$ . Further, to be visible from all vertices of the  
 663 other chain, it has to be to the left of the lines  $p_a l_{j+1}$  and  $p_b l_j$ . Let  $x_a$  be the apex of the triangle that  
 664 is defined by these constraints, and observe that  $x_a$  is the intersection of two of the four lines. We can  
 665 now add a chain of points on a circular arc inside the triangle  $l_j p_a x_a$ , as described above.

666 The coordinates are rational, and since every point can be constructed using only a constant number  
 667 of other points, the numerator and denominator of each point are polynomial.



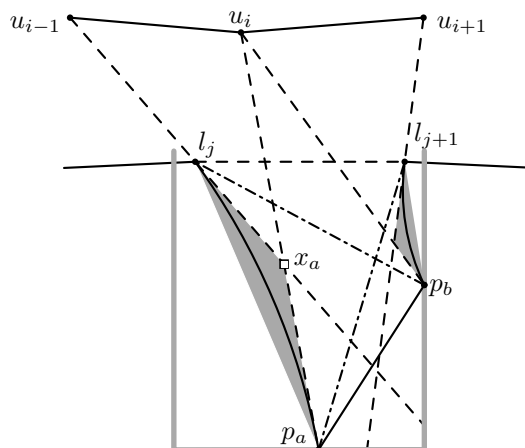


**Fig. 11** Construction of a small double chain for a sink.

### 668 A.3 General Position and Integer Coordinates

669 The ways in which a simple polygon can be triangulated is determined by the *order type* of the vertices,  
 670 i.e., the vector that indicates for each triple of vertices whether it is oriented clockwise or counterclock-  
 671 wise. Up to now, we did not care whether the point set is in general position, so there might also be  
 672 collinear point triples among vertices that are not directly related in the reduction. By simply multi-  
 673 plying all coordinates by all denominators used, we would obtain integer coordinates with exponential  
 674 values. To obtain integer coordinates bounded by a polynomial in the input size and a point set in  
 675 general position, we can use the following lemma.<sup>3</sup>

676 **Lemma A.1** *Let  $S$  be a point set with rational coordinates whose numerators and denominators have*  
 677 *absolute values of at most  $\xi$ . Then there is a point set  $S'$  with integer coordinates bounded by  $O(\xi^3)$*   
 678 *and a bijection between  $S$  and  $S'$  such that for every ordered triple of non-collinear points in  $S$ , the*  
 679 *orientation of the corresponding triple in  $S'$  is the same. In particular, if  $S$  is in general position, then*  
 680  *$S$  and  $S'$  have the same order type. Further,  $S'$  can be constructed in  $O(|S|^2)$  time.*

681 *Proof* Consider the set  $L$  of lines that are defined by all pairs of points of  $S$ . Choose  $\ell = q_1 q_2 \in L$  and  
 682  $p \in S \setminus \ell$  such that the horizontal distance  $v$  between  $p$  and  $\ell$  is minimal among all such distances (which  
 683 is non-zero as  $p$  is not on  $\ell$ ). Then  $v$  is rational, with numerator and denominator in  $O(\xi^2)$ . Further,  
 684 our choice required  $v > 0$ . When multiplying all  $x$ -coordinates by  $2/v$ , this distance is at least 2. The  
 685 basic idea is to round the  $x$ -coordinates. The crucial observation is that  $p$  has a  $y$ -coordinate that is  
 686 between the ones of  $q_1$  and  $q_2$ , as otherwise one of  $q_1$  and  $q_2$ , say,  $q_1$ , would be horizontally closer to  
 687 the line through  $p$  and  $q_2$ . For an ordered triple of points to change its orientation (from, say, clockwise  
 688 to counterclockwise), the horizontal distance between the point whose  $y$ -coordinate is between those  
 689 of the other two points would have to be reduced by more than 2. We can therefore safely round  
 690 the  $x$ -coordinates, which, in the worst case, reduces the horizontal distance between  $p$  and  $\ell$  by at  
 691 most 1. Hence, for every non-collinear ordered triple of points in  $S$ , the orientation of the corresponding

<sup>3</sup> The exact time bounds shown in the proof are irrelevant for the NP-hardness reduction (which even requires a different model of computation). We mention them only as they may be of general interest.

692 triple in the resulting point set is the same. We repeat the process analogously for the  $y$ -coordinates,  
 693 obtaining  $S'$ .

694 The horizontal or vertical distance  $v$  can easily be found by checking all triples of points. We can  
 695 improve this cubic time bound by considering the dual line arrangement  $\mathcal{A}$  of  $S$  (in which a point  
 696  $p = (x_p, y_p)$  corresponds to the dual line  $p^* : y = x \cdot x_p + y_p$ ). The dual arrangement can be constructed  
 697 in quadratic time [6, 8]. The shortest vertical distance in the primal corresponds to the shortest vertical  
 698 distance of a vertex and a side of a triangle defined by three dual lines. Clearly, the shortest distance  
 699 can only occur inside a triangle that is not intersected by another line.<sup>4</sup> Hence, we only need to test  
 700 the  $O(|S|^2)$  triangular cells of  $\mathcal{A}$ . □

701 Hence, if we construct the vertices with rational coordinates such that the vertices are in general  
 702 position, we can apply Lemma A.1 to have all vertices on the integer grid in general position.

703 General position can easily be obtained by applying a simple technique used in [19, Appendix A].  
 704 Observe first that the vertices of  $D$  are in general position. We take special care when placing the  $d - 1$   
 705 points of each chain of a sink gadget to not produce collinear points. Note that the final polygon  $P$  will  
 706 have  $|P| = 2(\beta n + 2) + 2N(d - 1)$  vertices. Instead of  $d - 1$  points, we choose  $2\binom{|P|}{2} + d - 1$  *candidate*  
 707 *points* on the circular arc for the chain. Consider any line through two already placed points. This line  
 708 intersects the circular arc in at most two points, so there are at most two candidate points that may  
 709 not be points of the double chain because of that line. As there are less than  $\binom{|P|}{2}$  such lines, there are  
 710 always enough candidate points left for selecting the  $d - 1$  points for the chain among them. Thus, the  
 711 vertices we obtain are in general position.

---

<sup>4</sup> Actually, any dual transform will do. When thinking of the rounding process as a continuous transformation, a change of the order type would involve a collapsing triangular cell of the dual arrangement, indicating a “close” point triple.